Large orders in strong-field QED

2006 J. Phys. A: Math. Gen. 39 11623

(http://iopscience.iop.org/0305-4470/39/37/018)

INSTITUTE OF PHYSICS PUBLISHING JOURNAL OF PHYSICS A: MATHEMATICAL AND GENERAL

J. Phys. A: Math. Gen. **39** (2006) 11623–11645 doi:10.1088/0305-4470/39/37/018

Large orders in strong-field QED

Thomas Heinzl[1] **and Oliver Schröder**[2]

[1] School of Mathematics and Statistics, University of Plymouth, Drake Circus, Plymouth PL4 8AA, UK
[2] Science + Computing ag, Hagellocher Weg 73, D-72070 Tübingen, Germany

E-mail: theinzl@plymouth.ac.uk and O.Schroeder@science-computing.de

Received 23 May 2006, in final form 25 July 2006
Published 29 August 2006
Online at stacks.iop.org/JPhysA/39/11623

Abstract

We address the issue of large-order expansions in strong-field QED. Our approach is based on the one-loop effective action encoded in the associated photon polarization tensor. We concentrate on the simple case of crossed fields aiming at possible applications of high-power lasers to measure vacuum birefringence. A simple next-to-leading order derivative expansion reveals that the indices of refraction increase with frequency. This signals normal dispersion in the small-frequency regime where the derivative expansion makes sense. To gain information beyond that regime we determine the factorial growth of the derivative expansion coefficients evaluating the first 82 orders by means of computer algebra. From this we can infer a nonperturbative imaginary part for the indices of refraction indicating absorption (pair production) as soon as energy and intensity become (super)critical. These results compare favourably with an analytic evaluation of the polarization tensor asymptotics. Kramers–Kronig relations finally allow for a nonperturbative definition of the real parts as well and show that absorption goes hand in hand with anomalous dispersion for sufficiently large frequencies and fields.

PACS numbers: 12.20.−m, 42.50.Xa, 42.60.−v

(Some figures in this article are in colour only in the electronic version)

1. Introduction

Recent years have seen a continuous progress in laser technology leading to ever increasing values of power and intensity. This is true for both optical lasers [1, 2] and systems based on free electrons such as the DESY vacuum ultraviolet free electron laser (VUV-FEL), a pilot system for the XFEL radiating in the x-ray regime [3]. High intensities imply strong electromagnetic fields which approach magnitudes such that vacuum polarization effects may

no longer be ignored even at the comparatively low photon energies involved (1 eV–10 keV). The theory describing these effects is strong-field quantum electrodynamics (QED).

The most exciting and therefore best-studied effect arises when the ubiquitous virtual electron–positron pairs become real (Schwinger pair production [4]). This happens if the energy gain of an electron across a Compton wavelength $\bar{\lambda}_e$ equals its rest energy m_e implying a critical electric field

$$E_c \equiv \frac{m_e^2}{e} \simeq 1.3 \times 10^{18}\ \mathrm{V\,m^{-1}}. \tag{1}$$

This also is often named after Schwinger although it has first been obtained by Sauter upon solving the Dirac equation in a homogeneous electric field [5].

The physical situation to be analysed in this paper is as follows. We assume a background field consisting of an intense, focused laser beam of optical frequency $\Omega \simeq 1\ \mathrm{eV} \ll m_e$. The associated gauge potential and field strengths are denoted by A_μ and $F_{\mu\nu}$, respectively. The laser beam configuration is modelled by *crossed fields* with electric and magnetic fields constant, orthogonal and of the same magnitude,

$$E = B \equiv F = \text{const}, \qquad \boldsymbol{E} \perp \boldsymbol{B}. \tag{2}$$

This configuration may be viewed as the zero-frequency limit of a plane wave, $\Omega \to 0$. In covariant notation one may write

$$A_\mu = \tfrac{1}{2} F_{\mu\nu} x^\nu, \tag{3}$$

with, for instance, $F_{01} = F = -F_{31}$ and all other (independent) entries vanishing. Working with crossed fields leads to enormous simplifications as will be seen below.

The crossed-field configuration will be probed by a weak plane-wave field encoded in the potential a_μ and field strength $f_{\mu\nu} = \partial_\mu a_\nu - \partial_\nu a_\mu$. We denote the probe wave vector by

$$k = \omega(1, n\mathbf{k}), \tag{4}$$

where $n \geqslant 1$ represents the index of refraction ($n = 1$ *in vacuo*) and the unit vector $\mathbf{k}$ the direction of propagation. Note that $n = 1/v$ with $v = \omega/|\boldsymbol{k}| \leqslant 1$ being the phase velocity of the probe propagating through the modified vacuum. This set-up has recently been suggested for an experiment to measure vacuum birefringence for the first time [6].

The corrections to pure Maxwell theory to leading order in the fluctuation a_μ are given by the effective action [7]

$$\delta S \equiv \frac{1}{2} \int \mathrm{d}^4x\, \mathrm{d}^4y\, a_\mu(x) \Pi^{\mu\nu}(x, y; A) a_\nu(y). \tag{5}$$

This is basically determined by the polarization tensor (or photon self-energy) $\Pi^{\mu\nu}$ in the presence of the background field A_μ.

In one-loop approximation the polarization tensor is represented by the Feynman diagram

$\Pi_{\mu\nu} =$  (6)

where the heavy lines denote the fermion propagator dressed by the background field A (dashed lines below),

$S_F[A] \equiv$  (7)

Obviously, the first term on the right-hand side in (7) corresponds to vanishing background fields, $A = 0$. In terms of the dressed propagator S_F the polarization tensor (in momentum

space) is given by the integral

$$\Pi^{\mu\nu}(k;A) = -\mathrm{i}e^2\,\mathrm{tr}\int\frac{\mathrm{d}^4p}{(2\pi)^4}\gamma^\mu S_F(p)\gamma^\nu S_F(p-k), \tag{8}$$

where 'tr' denotes the Dirac trace.

The dressed propagator and the associated one-loop polarization tensor are known exactly for a few special backgrounds only (see [8] and [9] for overviews). In particular, an exact solution is available for the crossed fields (2) due to Narozhnyi [10] and Ritus [11] (for a generalization to plane waves, see [12]). Their results may be written somewhat symbolically in terms of a spectral decomposition,

$$\Pi^{\mu\nu}(k;A) = \sum_{i=0,\pm}\Pi_i(k;A)\epsilon_i^\mu\epsilon_i^\nu, \tag{9}$$

with three orthogonal eigenvectors $\epsilon_i = \epsilon_i(k;A)$ satisfying $\epsilon_i\cdot k = 0$. The eigenvalues Π_i are given by somewhat complicated double integrals, the explicit form of which will be given below. It is important to note that the representation (9) is valid for arbitrary external field strength and probe frequency. In other words, it contains all orders in the background intensity and probe energy.

Let us briefly get an idea of the orders of magnitude involved. We assume that our probe is provided by another laser, possibly of high frequency, i.e. $\omega \gg \Omega$. For instance, if we think of the projected DESY XFEL as a probe with a projected wave length of $\lambda = 0.1$ nm, hence $\omega \simeq 10$ keV, we expect a ratio $\omega/m_e \simeq 0.02 \ll 1$, that is *low energy* also for the probe. About the same frequencies can be achieved for photons from a laser-based Thomson back-scattering source [13].

Assuming the background as an optical Petawatt laser focused down to the diffraction limit the peak intensity will be [2, 14]

$$I = P/\Lambda^2\pi \simeq 3\times10^{22}\ \mathrm{W\,cm^{-2}}, \tag{10}$$

for wavelength $\Lambda = 2\pi/\Omega \simeq 1\,\mu$m and power $P = 1$ PW. Sauter's critical field (1) corresponds to an intensity of

$$I_c = E_c^2 = m_e^4/e^2 \simeq 4\times10^{29}\ \mathrm{W\,cm^{-2}}, \tag{11}$$

still seven orders of magnitude larger than (10) implying *low intensity* for our background laser[3]. Hence for present technology we have two primary small parameters [6, 15], namely

$$\nu^2 \equiv \omega^2/m_e^2 \lesssim 4\times10^{-4}, \tag{12}$$

$$\varepsilon^2 \equiv E^2/E_c^2 = I/I_c \simeq 1\times10^{-7}. \tag{13}$$

We have listed the squared values as these typically arise as the leading-order (LO) contributions the reasons being essentially Lorentz and gauge invariance.

In view of the small parameters (12) and (13) it seems safe to assume that LO accuracy in ν^2 and ϵ^2 will suffice for the time being. Anticipating further increase in laser power [1] we will, however, also consider higher orders in this paper and confront the outcome numerically with the exact (albeit implicit) one-loop results. This should provide some intuition about the limitations of derivative and weak-field expansions in cases where exact results are not available and one has to rely entirely on the accuracy of the expansions.

[3] While the presently attainable fields are 'weak' compared to the critical field they are certainly very strong by everyday standards. In particular they exceed *static* lab magnetic fields by orders of magnitude. This justifies the phrase 'strong-field QED' in the title.

The paper is organized follows. We first go through a general (mainly algebraic) discussion of the polarization tensor where we also give the integral representations. Section 3 discusses the next-to-leading (NLO) results while section 4 extends these to order 80. Our findings are then compared with an asymptotic analysis of the integral representations in section 5. We finally present our conclusions in section 6.

2. General analysis of $\Pi^{\mu\nu}$

In order to evaluate (9) the following choice for the basis vectors ϵ_i has been suggested in [16],

$$b^\mu \equiv F^{\mu\nu}k_\nu, \tag{14}$$

$$\tilde{b}^\mu \equiv \tilde{F}^{\mu\nu}k_\nu, \tag{15}$$

$$c^\mu \equiv F^{\mu\nu}b_\nu, \tag{16}$$

where, as usual, $\tilde{F}^{\mu\nu} = (1/2)\epsilon^{\mu\nu\alpha\beta}F_{\alpha\beta}$ denotes the dual field strength. The first two basis vectors are obviously orthogonal to k,

$$b\cdot k = 0 = \tilde{b}\cdot k, \tag{17}$$

while the last one is not,

$$c\cdot k = -b^2. \tag{18}$$

However, if we follow [11] and define

$$d^\mu \equiv \left(g^{\mu\nu} - \frac{k^\mu k^\nu}{k^2}\right)c_\nu \equiv \mathbb{P}^{\mu\nu}c_\nu \equiv -\frac{1}{k^2}\epsilon^{\mu\nu\rho\sigma}k_\nu b_\rho \tilde{b}_\sigma, \tag{19}$$

the vectors b, $\tilde{b}$ and d constitute an orthogonal dreibein which satisfies

$$\frac{d^\mu d^\nu}{d^2} + \frac{\tilde{b}^\mu\tilde{b}^\nu}{b^2} + \frac{b^\mu b^\nu}{b^2} = \mathbb{P}^{\mu\nu}. \tag{20}$$

The spectral decomposition (9) may then be rewritten as

$$\Pi^{\mu\nu} = \Pi_0\frac{d^\mu d^\nu}{d^2} + \Pi_+\frac{\tilde{b}^\mu\tilde{b}^\nu}{b^2} + \Pi_-\frac{b^\mu b^\nu}{b^2}, \tag{21}$$

and coincides with the one used in the monograph [8]. The eigenvalues Π_i depend on all the independent invariants one can form from k^μ, the basis vectors and the background field strength. For crossed fields, however, most of these are either vanishing or dependent quantities. In particular, we have

$$\mathscr{S} \equiv -\tfrac{1}{4}F_{\mu\nu}F^{\mu\nu} = 0, \tag{22}$$

$$\mathscr{P} \equiv -\tfrac{1}{4}F_{\mu\nu}\tilde{F}^{\mu\nu} = 0. \tag{23}$$

We are thus left with only two basic invariants, k^2 and b^2, such that the eigenvalues in (21) can be written as a linear combination of those,

$$\Pi_i \equiv k^2 P(k^2, b^2) + \frac{b^2}{I_c}P_i(k^2, b^2), \qquad i = 0, \pm, \tag{24}$$

where P and P_i are dimensionless polynomials in k^2 and b^2 (see below). Note that the k^2-term is the same for all eigenvalues as it is the one surviving the limit of vanishing background ($b^2 \to 0$). According to (4) we have

$$k^2 = \omega^2(1 - n^2), \tag{25}$$

which is negative[4] in a modified vacuum ($n > 1$). To calculate b^2 we note that the Maxwell energy–momentum tensor for the crossed background fields is

$$T^{\mu\nu} = F^{\mu\lambda}F_{\lambda}{}^{\nu} - g^{\mu\nu}\mathscr{S} = F^{\mu\lambda}F_{\lambda}{}^{\nu}, \tag{26}$$

whereupon b^2 simply becomes

$$b^2(k) = -T^{\mu\nu}k_\mu k_\nu. \tag{27}$$

Using (4) again this translates into the expression

$$b^2 = -\omega^2[\mathcal{H}(1+n^2) - 2n\boldsymbol{S}\cdot\mathbf{k} - n^2\mathcal{H}_k], \tag{28}$$

where we have introduced the abbreviations

$$\mathcal{H} \equiv T^{00} = \tfrac{1}{2}(E^2 + B^2) = F^2, \tag{29}$$

$$S^i \equiv T^{0i} = \epsilon^{ijk}E^jB^k, \tag{30}$$

$$\mathcal{H}_k \equiv (\boldsymbol{E}\cdot\mathbf{k})^2 + (\boldsymbol{B}\cdot\mathbf{k})^2, \tag{31}$$

the first two of which represent the Maxwell energy–density and the Poynting vector, respectively. Note that both these quantities are directly related to the intensity,

$$\mathcal{H} = |\boldsymbol{S}| = I. \tag{32}$$

Expression (28) for b^2 coincides with the quantity z_k on p 21 of [8]. There is, however, an alternative expression which nicely illustrates the kinematics involved. Introducing the background 4-vector $K \equiv \Omega(1, \boldsymbol{K})$, $\boldsymbol{K}^2 = 1$ and assuming background gauge $\partial\cdot A = 0$ one finds

$$b^2 = b^2(\theta) = -\omega^2 I(1 - n\cos\theta)^2 \leqslant 0, \tag{33}$$

where θ is the angle between the probe and background directions ($\boldsymbol{k}$ and $\boldsymbol{K}$, respectively). Note that b^2 becomes independent of n for a perpendicular configuration implying $b^2(\pi/2) = -\omega^2 I$.

In order to obtain reasonably simple expressions for the coefficient functions P and P_i multiplying k^2 and b^2/I_c in (24) we follow [11] and trade the invariants k^2 and b^2 for the dimensionless parameters

$$\lambda \equiv k^2\big/m_e^2 = \nu^2(1-n^2) \leqslant 0, \tag{34}$$

$$\kappa^2 \equiv -b^2\big/I_c m_e^2 = \epsilon^2\nu^2(1-n\cos\theta)^2 \geqslant 0. \tag{35}$$

The eigenvalues of $\Pi^{\mu\nu}$ from (24) are then given by the expressions

$$\Pi_0(\lambda,\kappa^2) = m_e^2\lambda P(\lambda,\kappa^2), \tag{36}$$

$$\Pi_\pm(\lambda,\kappa^2) = \Pi_0(\lambda,\kappa^2) - m_e^2\kappa^2 P_\pm(\lambda,\kappa^2), \tag{37}$$

implying $P_0 = 0$ in particular. Using the integral representations given in [11] the remaining coefficient functions P and $P_\pm$ may be compactly written as

$$P(\lambda,\kappa^2) = P(\lambda,0) - \frac{2\alpha}{\pi}\int_0^1 \mathrm{d}x\, x\bar{x}\, f_1(z), \tag{38}$$

[4] Our metric is $g^{\mu\nu} = \mathrm{diag}(1,-1,-1,-1)$.

$$P(\lambda,0)=\frac{2\alpha}{\pi}\int_0^1 \mathrm{d}x\, x\bar{x}\ln(1-\lambda x\bar{x}), \tag{39}$$

$$P_\pm(\lambda,\kappa^2)=-\frac{\alpha}{3\pi}\kappa^{-4/3}\int_0^1 \mathrm{d}x\,\frac{2+(1\pm 3)x\bar{x}}{(x\bar{x})^{1/3}}f'(z). \tag{40}$$

In the above, we have introduced the Feynman parameters[5] x and $\bar{x}\equiv 1-x$ and the variable [11]

$$z=z(\lambda,\kappa,x)\equiv\frac{1-\lambda x\bar{x}}{(\kappa x\bar{x})^{2/3}}, \tag{41}$$

which is the argument of the auxiliary functions

$$f(z)\equiv \mathrm{i}\int_0^\infty \mathrm{d}t\,\mathrm{e}^{-\mathrm{i}zt-\mathrm{i}t^3/3}=\pi[\mathrm{Gi}(z)+\mathrm{iAi}(z)], \tag{42}$$

$$f_1(z)\equiv\int_0^\infty\frac{\mathrm{d}t}{t}\,\mathrm{e}^{-\mathrm{i}zt}(\mathrm{e}^{-\mathrm{i}t^3/3}-1). \tag{43}$$

f' denotes the derivative of f with respect to z; Gi and Ai are Scorer and Airy functions, respectively (see e.g. [17] or the digital library of mathematical functions [18]).

As both Gi and Ai are real for real arguments we can immediately infer from (40) and (42) that the eigenvalues $\Pi_\pm$ will develop imaginary parts determined by the Airy function $\mathrm{Ai}(z)$ in the integrand. It is thus natural to expect that also the index n of refraction will become complex, its imaginary part signalling absorption of photons by the vacuum. Of course, the only physical interpretation of this phenomenon is pair production.

Enormous simplifications arise naturally for vanishing external field, i.e. $\kappa^2=0$. In this case all eigenvalues become degenerate, $\Pi_i\equiv\Pi=m_e^2\lambda P$ and one just obtains Schwinger's one-loop expression for the photon self-energy [4] in the form

$$\Pi^{\mu\nu}=\Pi(k^2)\mathbb{P}^{\mu\nu}=m_e^2\lambda P(\lambda,0)\mathbb{P}^{\mu\nu}. \tag{44}$$

The scalar function $P(\lambda,0)$ is given in (39) and coincides with standard text book results obtained via covariant perturbation theory (see e.g. [19], chapter 7). For small momenta it becomes

$$P(\lambda,0)=-\frac{\alpha}{15\pi}\lambda+O(\lambda^2), \tag{45}$$

so that $\Pi(k^2)=O(k^4)$ for vanishing external field.

The next logical step is to expand the exponentials in (42) and (43) in powers of λ and κ^2. This amounts to a derivative expansion in the probe field (keeping the background fixed) and will be further pursued in the next section.

Before that let us conclude the general reasoning by determining the dispersion relations for k. Adopting a plane wave ansatz for the probe field, $f_{\mu\nu}=\mathrm{i}(k_\mu\epsilon_\nu-k_\nu\epsilon_\mu)\exp(\mathrm{i}k\cdot x)$, and adding the Maxwell term yields the wave equation

$$\Box^{\mu\nu}\epsilon_\nu\equiv-(k^2\mathbb{P}^{\mu\nu}-\Pi^{\mu\nu})\epsilon_\nu=0, \tag{46}$$

which has nontrivial solutions only if

$$\det\Box^{\mu\nu}(k)=0, \tag{47}$$

[5] The Feynman parameter x is related to the integration variables v in [8] and v in [11] via $v=2x-1$ and $v=1/x\bar{x}$, respectively. In particular, $\mathrm{d}v=(x-\bar{x})/(x\bar{x})^2\,\mathrm{d}x$.

i.e. if an eigenvalue of $\Box^{\mu\nu}$ vanishes,

$$k^2 - \Pi_i(k^2, b^2) \equiv h_i^{\mu\nu}(k^2, b^2)k_\mu k_\nu = 0. \tag{48}$$

Following [20, 21] we have introduce effective metrics $h_i^{\mu\nu}$ to make explicit that (48) represents 'modified light cone conditions' [8]. Inserting (24) the three metrics become

$$h_i^{\mu\nu}(\lambda, \kappa^2) = g^{\mu\nu}[1 + P(\lambda, \kappa^2)] + T^{\mu\nu}P_i(\lambda, \kappa^2)/I_c. \tag{49}$$

As $P_0 = 0$ the metric $h_0^{\mu\nu}$ is conformally flat,

$$h_0^{\mu\nu}(\lambda, \kappa^2) = g^{\mu\nu}[1 + P(\lambda, \kappa^2)], \tag{50}$$

and does not modify the light cone. Note in particular that in contrast to a plasma of real charges weak crossed fields do not generate a longitudinal photon so that $h_0^{\mu\nu}$ remains unphysical.

The other two metrics, however, are physical and nontrivial leading to a modified light propagation. As $h_1 \neq h_2$ this implies 'birefringence of the vacuum'. For vanishing external fields ($\kappa^2 = 0$) all metrics merge into the conformal metric $h_0^{\mu\nu}(\lambda, 0)$ which describes a standard light cone.

3. NLO derivative expansion for the probe

The integral representations (38)–(40) for the polarization tensor may be expanded in powers of λ and κ^2 which are both $O(\nu^2)$. This derivative expansion becomes particularly straightforward if we first expand in ν and only afterwards perform the integrals, a procedure adopted throughout sections 3 and 4. Thus, we first rewrite the derivative of (42) and the second function (43) in order to exhibit the dependence on κ and λ,

$$f'(z) = (\kappa x \bar{x})^{4/3} \int_0^\infty \mathrm{d}\tau\, \mathrm{e}^{\mathrm{i}\lambda x\bar{x}\tau} \exp(-\mathrm{i}\tau - i\kappa^2 x^2 \bar{x}^2 \tau^3/3), \tag{51}$$

$$f_1(z) = \int_0^\infty \frac{\mathrm{d}\tau}{\tau}\, \mathrm{e}^{\mathrm{i}\lambda x\bar{x}\tau}\, \mathrm{e}^{-\mathrm{i}\tau}(\exp(-\mathrm{i}\kappa^2 x^2 \bar{x}^2 \tau^3/3) - 1), \tag{52}$$

where $z = z(\lambda, \kappa, x)$ was defined in (41). Upon expanding the exponentials the integrals both over Feynman parameters and proper time become elementary so that the eigenvalues Π_i to $O(\nu^4)$ are found to be

$$\Pi_0/m_e^2 = -\frac{\alpha}{15\pi}\lambda^2 + \frac{\alpha}{105\pi}\lambda\kappa^2, \tag{53}$$

$$\Pi_+/m_e^2 = -\frac{7\alpha}{45\pi}\kappa^2 - \frac{\alpha}{15\pi}\lambda^2 - \frac{23\alpha}{315\pi}\lambda\kappa^2 - \frac{52\alpha}{945\pi}\kappa^4, \tag{54}$$

$$\Pi_-/m_e^2 = -\frac{4\alpha}{45\pi}\kappa^2 - \frac{\alpha}{15\pi}\lambda^2 - \frac{2\alpha}{45\pi}\lambda\kappa^2 - \frac{4\alpha}{135\pi}\kappa^4. \tag{55}$$

Note that only $\Pi_\pm$ have LO contributions, $\Pi_\pm = O(\kappa^2) = O(\nu^2)$, whereas $\Pi_0 = O(\lambda^2) = O(\nu^4)$. To proceed we specialize to a head-on collision for which birefringence becomes maximal, cf (33) and (35). In this case, $\boldsymbol{k}\cdot\boldsymbol{K} = -1$ so that κ^2 attains its maximum value,

$$\kappa^2 = \epsilon^2\nu^2(1+n)^2. \tag{56}$$

The nontrivial dispersion relations $\Box_\pm \equiv k^2 - \Pi_\pm = 0$ implicitly determine two nontrivial indices of refraction $n_\pm$ as functions of the small parameters ϵ^2 and ν^2. To solve the equations $\Box_\pm(n, \epsilon, \nu) = 0$ for the indices $n_\pm$ we write

$$n_\pm \equiv 1 + \Delta_\pm \equiv 1 + \frac{\alpha}{45\pi}\epsilon^2\delta_\pm. \tag{57}$$

The last expression takes into account that corrections to $n = 1$ are due to nonvanishing external field intensity ϵ^2 the coupling to which is $O(\alpha)$. The remainders $\delta_\pm$ are expected to be of order unity. For the value $\epsilon^2 = 10^{-7}$ from (13) the prefactor is of order 10^{-11} so that at present the deviations from $n = 1$ are extremely small. It hence remains an experimental challenge to really measure them [6, 22].

If we expand the deviations according to

$$\delta_\pm = \delta_{0\pm} + \delta_{2\pm}\nu^2 + O(\nu^4), \tag{58}$$

we find at LO in k^2 or ν^2, i.e. $O(\nu^0)$,

$$\delta_{0+} = \frac{14}{1 - 7\alpha\epsilon^2/45\pi} = 14\left\{1 + 7\frac{\alpha\epsilon^2}{45\pi} + O(\alpha^2\epsilon^4)\right\}, \tag{59}$$

$$\delta_{0-} = \frac{8}{1 - 4\alpha\epsilon^2/45\pi} = 8\left\{1 + 4\frac{\alpha\epsilon^2}{45\pi} + O(\alpha^2\epsilon^4)\right\}. \tag{60}$$

Note that the first terms on the right-hand side are exact to all orders in the intensity ϵ^2. An independent check of the LO results based on the Heisenberg–Euler Lagrangian will be performed in the appendix.

To the best of our knowledge, the coefficients of order ϵ^0 in (59) and (60) have first been obtained in Toll's thesis [23][6] and independently in [25, 26] (see also [7, 10, 27]). The NLO=$O(\nu^2)$ expressions are somewhat more complicated,

$$\delta_{2+} = \left(\frac{416}{21} - \frac{184\alpha}{45\pi} + \frac{392\alpha^2}{675\pi^2}\right)\frac{\epsilon^2}{(1 - 7\alpha\epsilon^2/45\pi)^4}, \tag{61}$$

$$\delta_{2-} = \left(\frac{32}{3} - \frac{64\alpha}{45\pi} + \frac{128\alpha^2}{675\pi^2}\right)\frac{\epsilon^2}{(1 - 4\alpha\epsilon^2/45\pi)^4}. \tag{62}$$

Again, these expressions are exact to all orders in ϵ^2. For later purposes it is useful to attach names to the different factors,

$$\delta_{2\pm} = c_{2\pm}(\alpha)\epsilon^2 s_{2\pm}(\alpha\epsilon^2). \tag{63}$$

According to (61) and (62) the $c_{2\pm}$ are polynomials in $\alpha/45\pi$ while the $s_{2\pm}$ have the series expansions

$$s_{2+} = 1 + \frac{28\alpha}{45\pi}\epsilon^2 + \frac{98\alpha^2}{405\pi^2}\epsilon^4 + O(\epsilon^6), \tag{64}$$

$$s_{2-} = 1 + \frac{16\alpha}{45\pi}\epsilon^2 + \frac{32\alpha^2}{405\pi^2}\epsilon^4 + O(\epsilon^6). \tag{65}$$

Note that both at LO and NLO the QED expansion parameter is actually $\alpha/45\pi \simeq 5 \times 10^{-5}$ rather than α itself. The coefficients $c_{2\pm}$ are dominated by the leading terms of $O(\alpha^0)$ which both have a positive sign. This implies that (at least to first nontrivial order in the derivative expansion) the indices of refraction increase with frequency so that we have normal (rather than anomalous) dispersion.

[6] As we have not been able to get hold of this unpublished work our statement is based on the notes [24] where the relevant figure of Toll's thesis is reproduced on p 33.

Summarizing the findings above we see the following pattern emerging. Each of the two indices of refraction has a derivative expansion in v^2,

$$n_\pm = 1 + \Delta_\pm = 1 + \frac{\alpha\epsilon^2}{45\pi}\sum_{l=0}^{\infty}\delta_{2l\pm}(\alpha,\epsilon)v^{2l}, \tag{66}$$

where the δ_{2l} can be factorized by generalizing (63),

$$\delta_{2l\pm} \equiv c_{2l\pm}(\alpha)\epsilon^{2l}s_{2l\pm}(\alpha\epsilon^2/45\pi). \tag{67}$$

Hence, the different coefficient functions have the generic behaviour

$$\delta_{2l} = O(\epsilon^{2l}), \tag{68}$$

$$c_{2l} = 1 + O(\alpha), \tag{69}$$

$$s_{2l} = 1 + O(\alpha\epsilon^2), \tag{70}$$

for both subscripts $\pm$. Keeping only the leading orders in α in (67), i.e. $\delta_{2l} \simeq c_{2l}(0)\epsilon^{2l}$, results in a compact expression for the NLO derivative expansion,

$$\delta_\pm = 11 \pm 3 + \frac{320 \pm 96}{21}\epsilon^2v^2 + O(\alpha) + O(\alpha\epsilon^2). \tag{71}$$

Again, the relative plus sign between the first and second terms signals normal dispersion. Extrapolating (71) to all orders adopting the same approximations we expect (58) to become a function of ϵv only,

$$\delta \simeq \sum_{l=0}^{\infty} c_{2l}(0)(\epsilon v)^{2l}. \tag{72}$$

If we have a closer look at the coefficients $c_{0\pm}$ and $c_{2\pm}$ (at $O(\alpha^0)$) we see that they actually increase, the ratios being almost the same for both indices,

$$\frac{c_{2+}}{c_{0+}} \simeq \frac{416/21}{14} \simeq 1.4 \qquad \text{and} \qquad \frac{c_{2-}}{c_{0-}} \simeq \frac{32/3}{8} \simeq 1.3. \tag{73}$$

This is a first hint that our expansion in v (or ϵv) is only asymptotic which has to be expected upon comparing with closely related derivative expansions of effective actions [9, 28]. In the remainder of the paper we will investigate this issue in detail.

4. Large-order derivative expansion for the probe

Given the present day power of computer algebra systems we have decided to actually check whether normal dispersion persists beyond NLO in the derivative expansion. The answer is affirmative as shown in the `Mathematica` plots of figures 1 and 2. They display the second, sixth and tenth order in the derivative expansion of $\Delta = n - 1$ as a function of v at fixed background intensity $\epsilon^2 = 0.1$. The LO results (59) and (60) are given by the common intercept of the different graphs. One clearly identifies normal dispersion and a tendency for the curves to diverge with increasing order.

As already stated the results of the preceding section indicate strongly that the expansion (66) of the index of refraction is asymptotic both in frequency and intensity. Hence, for both the derivative and weak (external) field expansions we expect *factorial growth* of the expansion coefficients at large orders.

To test this expectation numerically we expand $\Delta_\pm$ in accordance with (66),

$$\Delta_\pm(v,\epsilon) = \frac{\alpha\epsilon^2}{45\pi}\sum_{l\geqslant 0}\delta_{2l\pm}(\epsilon)v^{2l}, \tag{74}$$

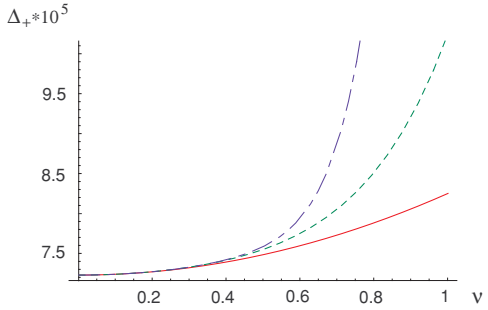

Figure 1. Higher order results for the deviation Δ_+ of the index n_+ from unity as a function of $\nu = \omega/m_e$ at fixed background intensity $\epsilon^2 = 0.1$. Full line: second order; short-dashed line: sixth order; long-dashed line: tenth order.

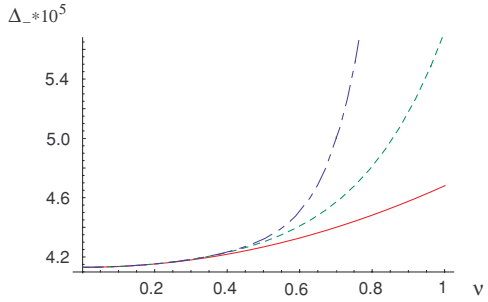

Figure 2. Same as figure 1 for Δ_-.

with $\delta_{2l\pm}$ as given in (67) and form the ratio[7]

$$r_{2l\pm} \equiv \frac{\delta_{2l+2,\pm}}{\epsilon^2 \delta_{2l\pm}} = \frac{c_{2l+2,\pm}(0)}{c_{2l,\pm}(0)}[1 + O(\alpha) + O(\alpha\epsilon^2)]. \tag{75}$$

The coefficients can (in principle) be determined by expanding the integral representations (38)–(40) using the auxiliary functions (42) and (43) (see the next section). For simple factorial growth, $\delta_{2l} \sim \Gamma(l)$, r_{2l} would depend linearly on l.

In what follows we want to ask the question what can be said about the factorial growth *without* using any knowledge of the special functions (42) and (43). That is, we perform a brute-force derivative expansion before calculating any integrals, trying to extend the method of the previous section to orders as large as possible to gain a maximum of information. The philosophy behind is our expectation that for realistic backgrounds such as laser fields this type of derivative expansion will be one of the main tools when analytical methods are not available. We thus expect our method to provide results complementary to numerical approaches like world-line Monte Carlo [30–33].

In order to extract the asymptotic behaviour of δ_{2l} or r_{2l} with high accuracy it is obviously desirable to go to the largest orders possible. Again, this is only feasible with the aid of computer algebra and was performed with an optimized `Mathematica` routine. Using a standard desktop PC we were able to achieve a maximal order of $2l = 82$. The determination of all $82/2$ coefficients for a given value ϵ^2 of intensity takes about an hour.

[7] We thank Paul Rakow for bringing this idea to our attention [29].

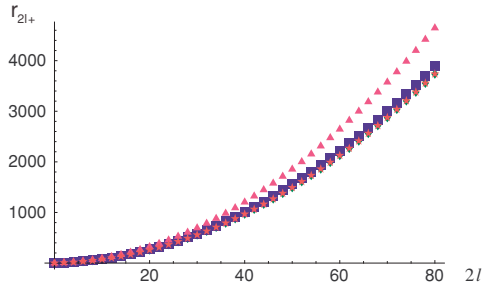

Figure 3. Successive coefficient ratio r_{2l+} as a function of order $2l$ for four different intensities, $\epsilon^2 = 0.1$ (♦), $\epsilon^2 = 1$ (★), $\epsilon^2 = 100$ (■) and $\epsilon^2 = 500$ (▲).

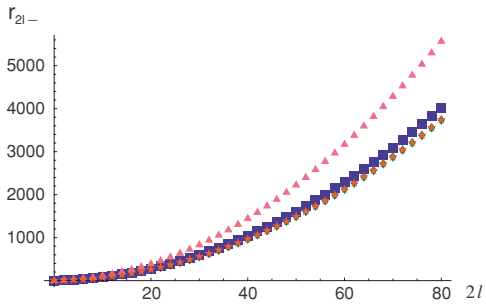

Figure 4. Successive coefficient ratio r_{2l-} as a function of order $2l$ for four different intensities, $\epsilon^2 = 0.1$ (♦), $\epsilon^2 = 1$ (★), $\epsilon^2 = 100$ (■) and $\epsilon^2 = 500$ (▲).

In figures 3 and 4 we have plotted the ratio (75) as a function of order $2l$ for different values of the intensity ϵ^2 ranging from 0.1 (subcritical) to 500 (supercritical).

One notes the following: first, the ϵ-dependence of r_{2l} is rather weak as expected from the discussion in the preceding section and the second expression in (75). To recognize corrections to the leading behaviour which is independent of ϵ one has to go to very large intensities and/or orders. For instance, the graphs for $\epsilon^2 = 0.1$ and $\epsilon^2 = 1$ basically are on top of each other. One needs $\epsilon = O(10^2)$ to see 10% deviations from the graphs with small ϵ values. This is consistent with the coefficients of ϵ^2 in (75) being of order 10^{-3}, cf (64) and (65).

Second, and more importantly, the ratio r_{2l} seems to depend quadratically on l which is simply explained by an asymptotic behaviour $\delta_{2l} \sim \Gamma(2l)$. Let us try to perform a more quantitative analysis. The following general ansatz

$$c_{2l}(0) = \rho^{2l}[\Gamma(2l - \sigma) + \tau\Gamma(2l - \sigma - 1)], \tag{76}$$

which is tailored after examples where exact results are available [28, 34], implies a ratio

$$r_{2l} = \rho^2[(2l)^2 + (1 - 2\sigma)2l + \sigma^2 - \sigma - 2\tau] \equiv a_2(2l)^2 + a_1 2l + a_0. \tag{77}$$

Fitting the curves of figures 3 and 4 to quadratic polynomials we find the a_i values listed in table 1.

The errors have been estimated by also fitting higher-order polynomials and monitoring the change in the coefficients. For all fits an extrapolation to $l \to \infty$ has been performed using Laurent series techniques.

Table 1. Fitted values for the polynomial coefficients in (77).

	$\epsilon^2 = 0.1$	$\epsilon^2 = 1$	$\epsilon^2 = 100$	$\epsilon^2 = 500$
a_{2+}	0.562 56(11)	0.562 95(35)	0.607(11)	0.8383(38)
a_{1+}	1.6892(29)	1.6899(49)	1.817(44)	2.51(42)
a_{0+}	1.691(41)	1.693(46)	1.69(27)	1.4(2.5)
a_{2-}	0.562 535(27)	0.562 75(15)	0.5865(15)	0.699(11)
a_{1-}	1.687 41(46)	1.687 95(16)	1.7591(21)	2.10(15)
a_{0-}	1.3926(36)	1.3928(70)	1.38(13)	1.25(90)

Table 2. Numerical values for the polynomial coefficients in (76).

	$\epsilon^2 = 0.1$	$\epsilon^2 = 1$	$\epsilon^2 = 100$	$\epsilon^2 = 500$
ρ_+	0.750 04(15)	0.750 30(47)	0.779(14)	0.9156(42)
σ_+	−1.0014(23)	−1.009(34)	−0.9967(91)	−1.00(24)
τ_+	−0.501(65)	−0.502(69)	−0.40(35)	0.2(2.2)
ρ_-	0.750 023(36)	0.750 17(20)	0.7658(20)	0.836(13)
σ_-	−0.999 83(34)	−0.999 73(26)	−0.9997(20)	−1.002(84)
τ_-	−0.2380(52)	−0.238(12)	−0.18(22)	0.11(99)

Via (77) the values of table 1 translate into the asymptotic coefficients ρ, σ and τ introduced in (76) as listed in table 2.

One notes that, for small intensities, both ρ and σ are the same for the two indices of reflection, i.e. $\rho_+ = \rho_- \equiv \rho$ and $\sigma_+ = \sigma_- \equiv \sigma$ while $\tau_+ \neq \tau_-$. Furthermore, σ seems to be independent of intensity (unlike ρ and τ). We can even guess the following 'analytic' values for ρ and σ,

$$\rho = 3/4, \qquad \text{and} \qquad \sigma = -1. \tag{78}$$

For $\epsilon^2 \lesssim 1$ these values for ρ and σ should be quite accurate. Not unexpectedly, the largest errors reside in the subleading coefficients $\tau_\pm$. In view of this we refrain from any further guesses and just quote the τ-values of table 2.

We conclude this numerical discussion with two remarks. First, one may ask whether the quadratic behaviour (77), which seems to work so well, can be confirmed by doing an unbiased fit to the leading asymptotics of the form

$$c_{2l}(0) = \rho^{2l}\Gamma(\beta l - \sigma), \tag{79}$$

rather than using (76). For the 'plus' case and the two extreme intensities, $\epsilon^2 = 0.1$ and $\epsilon^2 = 500$, we have checked that quadratic behaviour (i.e. $\beta = 2$) is indeed obtained with a relative error of less than 10^{-3}. The fit is somewhat better for the low intensity as compared to the large one, the residual mean squares being 0.043 and 0.30, respectively.

Second, with an eye towards realistic backgrounds like lasers, one may ask how many orders need to be minimally included to make statements about the asymptotics. We have therefore investigated the dependence of the fit parameters on the highest order $2l$ included in the fit. This dependence is displayed in figure 5 which shows the relative difference,

$$R_i \equiv \frac{a_{i+}(2l) - a_{i+}(82)}{a_{i+}(2l) + a_{i+}(82)}, \qquad i = 0, 1, 2, \quad 8 \leqslant 2l \leqslant 80, \tag{80}$$

as a function of the maximum order $2l$ included, for two values of intensity (left: intensity $\epsilon^2 = 0.1$; right: $\epsilon^2 = 500$.). The sizes of the plot symbols are chosen such that the relative

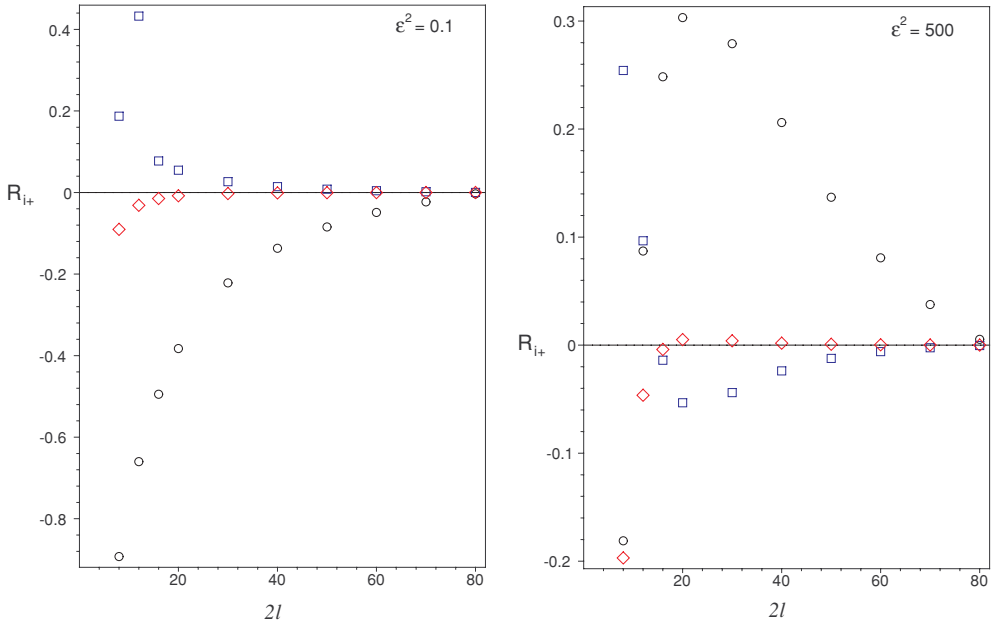

Figure 5. Behaviour of the fit coefficients a_2 ($\diamond$), a_1 ($\square$) and a_0 ($\circ$) as a function of the maximal order $2l$ employed for their determination relative to their values at $2l = 82$ (represented by the null line). Left: intensity $\epsilon^2 = 0.1$. Right: intensity $\epsilon^2 = 500$.

difference R_i drops below 1% as soon as the symbol touches the null line representing our best fit with $2l = 82$. To determine the leading (quadratic) coefficient a_2 to this accuracy about 20 orders in ω, hence 10 orders in the actual expansion parameter ω^2, seem sufficient. For the subleading coefficients, one has to go to orders $2l$ of 40 and 80, respectively (for intensity 0.1). This tendency gets worse if the intensity increases. For the leading coefficient encoded in R_2, the intensity dependence is rather weak.

With all coefficients being safely determined let us plug the asymptotic ansatz (76) into the expansion (74) adopting the approximation (67) so that the expansion parameter becomes $\epsilon\nu$ rather than ν. This should be fine for $\epsilon^2 \lesssim 1$. As our ansatz (76) is supposed to hold only asymptotically for large orders we cannot expect to describe the low orders accurately. We nevertheless proceed by eliminating the Gamma functions using the integral expression

$$\rho^z \Gamma(z) = \int_0^\infty \mathrm{d}s \frac{\mathrm{e}^{-1/\rho s}}{s^{z+1}}. \tag{81}$$

This transforms the required summations over l into geometric series and yields the following integral representation for (74),

$$\Delta_\pm(\epsilon, \nu) = N_\pm \frac{\alpha\epsilon^2}{45\pi} \int_0^\infty \mathrm{d}s \frac{s}{s^2 - (\epsilon\nu)^2} [(\rho s)^\sigma + \tau_\pm (\rho s)^{\sigma+1}] \, \mathrm{e}^{-1/\rho s}, \tag{82}$$

where we have allowed for an undetermined scale $N_\pm$. As it stands the integral is ambiguous as there are poles on the real axis. The left-hand side may be viewed as originating from the derivative (or $\epsilon\nu$) expansion which has real coefficients. It is therefore tempting to interpret (82) as the following dispersion integral (see e.g. [35], chapter 18),

$$\mathrm{Re}\ \Delta_\pm(\epsilon\nu) = N_\pm \frac{2}{\pi} \mathfrak{P} \int_0^\infty \mathrm{d}s \frac{s}{s^2 - (\epsilon\nu)^2} \ \mathrm{Im}\ \Delta_\pm(s), \tag{83}$$

where the pole ambiguity has been resolved in terms of the Cauchy principal value denoted by $\mathfrak{P}$. The right-hand side contains a 'nonperturbative imaginary part' [34],

$$\operatorname{Im}\Delta_\pm(\epsilon\nu) = N_\pm \frac{\alpha\epsilon^2}{90}(\epsilon\nu\rho)^\sigma(1+\tau_\pm\epsilon\nu\rho)\,\mathrm{e}^{-1/\epsilon\nu\rho}, \tag{84}$$

i.e. an exponential that cannot be obtained from a perturbative expansion in $\epsilon\nu$. Inserting the universal values (78) and $\tau_\pm$ from table 2 this becomes

$$\operatorname{Im}\Delta_\pm(\epsilon\nu) = N_\pm \frac{\alpha\epsilon^2}{90}\frac{4}{3\epsilon\nu}\left(1-\frac{3\epsilon\nu}{4}\begin{Bmatrix}0.50\\0.24\end{Bmatrix}\right)\mathrm{e}^{-4/3\epsilon\nu}. \tag{85}$$

Note that the small parameter involved seems to be $3\epsilon\nu/4$.

Summarizing we can say that our large-order derivative expansion has provided us with a quantitative formula for the asymptotics of the series which by means of (83) could be turned into a statement about the nonperturbative imaginary part. As already stated, this should be directly related to absorption and pair production. In what follows we will check our findings by an analytic discussion of the integral representations of the eigenvalues Π_i, in particular of (40).

5. Analytic results

Proceeding analytically is equivalent to analysing the (derivative of the) auxiliary function $f(z)$ introduced in (42). The leading orders for both weak and strong external fields have already been investigated by Narozhnyi [10] (see also [36]). In this section we want to go further and discuss arbitrary large orders in the low-frequency, weak-field expansion of the eigenvalues Π_i. Nevertheless, to keep things manageable we follow Narozhnyi's example and adopt an approximation that leads to substantial simplifications. Namely, we neglect vacuum modifications *in expressions involving the eigenvalues* $\Pi_i(\lambda,\kappa)$ by setting $n=1$ or, equivalently, $\lambda=0$ in their arguments. From (36) and (37) we thus have the approximate identities

$$\Pi_0(\lambda,\kappa^2) \simeq \Pi_0(0,\kappa^2) = 0, \tag{86}$$

$$\Pi_\pm(\lambda,\kappa^2) \simeq \Pi_\pm(0,\kappa^2) = -m_e^2\kappa^2 P_\pm(0,\kappa^2). \tag{87}$$

According to (56) we have in the same approximation,

$$\kappa \simeq 2\epsilon\nu, \tag{88}$$

which turns our eigenvalues into functions of the product $\epsilon\nu$ in line with our discussion of the previous section. The upshot of all this is that the dispersion relations (48) simplify drastically so that one is left with the task to determine $P_\pm$ in

$$\Delta_\pm(\kappa,\lambda) \simeq \Delta_\pm(\epsilon\nu) \simeq 2\epsilon^2 P_\pm(\epsilon\nu). \tag{89}$$

As an aside we remark that according to (33), (34) and (35) Narozhnyi's approximation is expected to be particularly good if probe and background are perpendicular as b^2 and hence κ are indeed independent of n in this case[8]. The perpendicular set-up has recently been suggested as a means to look for 'vacuum diffraction' [37].

To evaluate (89) we want to calculate $P_\pm$ as a power series in $\epsilon\nu$ using the integral representation (40). From the definition of κ^2 in (35) or (88) and of $z(\lambda,\kappa,x\bar{x})$ in (41) it is clear that an expansion in $\epsilon\nu$ corresponds to determining the large-z asymptotics of

$$f'(z) = \pi\,\mathrm{Gi}'(z) + \mathrm{i}\pi\,\mathrm{Ai}'(z), \tag{90}$$

[8] with the replacement $2\epsilon\nu \to \epsilon\nu$ understood in (88).

which appears in the integrand of (40). Using asymptotic expansions for $\mathrm{Ai}(z)$ given in [17] and $\mathrm{Gi}(z)$ in [38] one obtains for (90)

$$f'(z) = -\frac{1}{z^2} - \frac{1}{z^5}\sum_{k=0}^{\infty}\frac{g_k}{z^{3k}} - \frac{\mathrm{i}}{2}\pi^{1/2}z^{1/4}\,\mathrm{e}^{-\zeta}\sum_{k=0}^{\infty}(-1)^k A_k \zeta^{-k}, \tag{91}$$

with the abbreviations

$$\zeta \equiv \frac{2}{3}z^{3/2}, \tag{92}$$

$$g_k \equiv \frac{(3k+4)\Gamma(3k+3)}{3^k\Gamma(k+1)}, \tag{93}$$

$$A_k \equiv -\frac{6k+1}{6k-1}\frac{\Gamma(3k+1/2)}{54^k k!\Gamma(k+1/2)}. \tag{94}$$

The expression (91) now has to be plugged in the integral (40). Throughout the subsequent calculations we use Narozhnyi's approximation which implies

$$z \simeq (\kappa x\bar{x})^{-2/3}, \qquad \zeta \simeq 2/3\kappa x\bar{x}. \tag{95}$$

In what follows we will separately calculate the real and imaginary parts of $P_\pm$.

5.1. Calculation of the real part

Using (88), (95) and the integral representation of the Beta function,

$$\int_0^1 \mathrm{d}x\, x^{n-1}\bar{x}^{m-1} = B(n,m) = \frac{\Gamma(n)\Gamma(m)}{\Gamma(n+m)}, \tag{96}$$

the real part of $P_\pm$ can be obtained in closed form,

$$\mathrm{Re}\,P_\pm(\kappa) = \frac{\alpha m^2}{3\pi}\sum_{l\geqslant 0} G_l \kappa^{2l}\{2B(2l+2,2l+2) + (1\pm 3)B(2l+3,2l+3)\}. \tag{97}$$

Here, we have introduced the new expansion coefficients

$$G_l \equiv \begin{cases} 1, & l = 0 \\ g_{l-1}, & l > 0. \end{cases} \tag{98}$$

The leading term ($l = 0$) in the expansion (97) yields for (89)

$$\Delta_\pm(\epsilon\nu) = 2\epsilon^2 P_\pm(\epsilon\nu) \simeq (11\pm 3)\frac{\alpha\epsilon^2}{45\pi}, \tag{99}$$

which reassuringly is consistent with (71).

It is the presence of the Beta functions in (97) that causes factorial growth. To analyse this in the spirit of the previous section we expand the corrections to the indices of refraction according to (66) and (72),

$$\mathrm{Re}\,\Delta_\pm \equiv 2\epsilon^2\,\mathrm{Re}\,P_\pm = \frac{\alpha\epsilon^2}{45\pi}\sum_{l\geqslant 0} c_{2l,\pm}(0)(\epsilon\nu)^{2l}. \tag{100}$$

Comparing with (97) we find the coefficient ratios

$$r_{2l\pm} = 4\frac{G_{l+1}}{G_l}\frac{2B(2l+4,2l+4) + (1\pm 3)B(2l+5,2l+5)}{2B(2l+2,2l+2) + (1\pm 3)B(2l+3,2l+3)}. \tag{101}$$

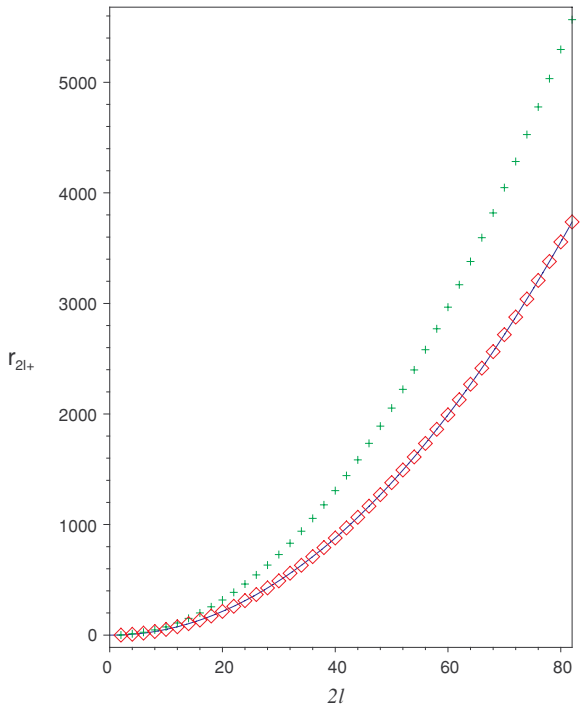

Figure 6. Coefficient ratio r_{2l+} as a function of order $2l$. Diamonds: numerical values for $\epsilon^2 = 0.1$; crosses: numerical values for $\epsilon^2 = 500$ (both as in figure 3); full line: analytical ratio from (101).

These can be evaluated exactly to give

$$r_{2l+} = \frac{2(6l+13)(3l+4)(3l+2)(2l+3)(l+1)}{(6l+7)(4l+9)(4l+7)} = \frac{9}{16}(2l)^2 + \frac{54}{32}2l + \frac{452}{256} - \frac{372}{256}\frac{1}{2l} + O(1/l^2), \tag{102}$$

$$r_{2l-} = \frac{(6l+14)(3l+2)(2l+3)(l+1)}{(4l+9)(4l+7)} = \frac{9}{16}(2l)^2 + \frac{54}{32}2l + \frac{356}{256} - \frac{12}{256}\frac{1}{2l} + O(1/l^2). \tag{103}$$

Obviously, as the $r_{2l\pm}$ are independent of intensity they cannot describe all curves of figures 3 and 4 which, after all, *are* intensity dependent. However, we expect good agreement between numerical and analytical values of $r_{2l\pm}$ for small intensities $\epsilon^2 \lesssim 1$. This is nicely corroborated by the graphs of figure 6 where the results for $\epsilon^2 = 0.1$ are on top of each other for all values of $2l$. This near-perfect agreement is due to the fact that upon neglecting the ϵ dependence of the coefficients (67) (and within Narozhnyi's approximation) *all* expansion coefficients are basically factorials, cf (97).

Matching (102) and (103) with (77) we read off the coefficients

$$a_2 = \tfrac{9}{16} = 0.5625, \tag{104}$$

$$a_1 = \tfrac{54}{32} = 1.6875, \tag{105}$$

$$a_{0+} = \tfrac{452}{256} = 1.765\,625, \tag{106}$$

$$a_{0-} = \tfrac{356}{256} = 1.390\,625, \tag{107}$$

which compare favourably with the entries of table 1 for $\epsilon^2 \lesssim 1$. The a_i translate exactly into the asymptotic parameters $\rho = 3/4$ and $\sigma = -1$ we had guessed in (78) while the τ-parameters become

$$\tau_+ = -\tfrac{41}{72} = -0.5694, \tag{108}$$

$$\tau_- = -\tfrac{17}{72} = -0.2361. \tag{109}$$

Again, these agree satisfactorily with the entries of table 2 for small ϵ, in particular for subscript 'minus'.

It remains to rewrite our nonperturbative imaginary part (85) by replacing the numerical $\tau_\pm$ by their analytic counterparts just obtained,

$$\operatorname{Im}\Delta_\pm(\epsilon\nu) = N_\pm \frac{\alpha\epsilon^2}{90}\frac{4}{3\epsilon\nu}\left(1 - \frac{3\epsilon\nu}{4}\frac{29 \pm 12}{72}\right)\mathrm{e}^{-4/3\epsilon\nu}. \tag{110}$$

Let us finally try to check this by a direct calculation of the imaginary part.

5.2. *Calculation of the imaginary part*

The determination of the imaginary part of $P_\pm$ is more involved as the integrand (40) contains an exponential that cannot be expanded in powers of $x\bar{x}$. Explicitly, the integrand is of the form

$$\mathrm{e}^{-\zeta}(x\bar{x})^n \simeq \exp(-2/3\kappa x\bar{x})(x\bar{x})^n, \tag{111}$$

which is to be integrated from 0 to 1. In order to proceed analytically we note that the product $x\bar{x}$ is peaked at the value $1/4$. Thus, it seems feasible to perform the integral via saddle point approximation which results in the formula

$$I(a,b) \equiv \int_0^1 \mathrm{d}x\,\mathrm{e}^{-ax\bar{x}}(x\bar{x})^b \simeq \left(\frac{\pi}{16a+4b}\right)^{1/2} 4^{-b}\,\mathrm{e}^{-4a}. \tag{112}$$

Here, the first prefactor has been obtained by extending the integration to the whole real axis in order to have a Gaussian integral. In our case, the parameters a and b are given by

$$a = 2/3\kappa \simeq 1/3\epsilon\nu \qquad \text{and} \qquad b = k \pm 1/2, \qquad k = 0, 1, 2, \ldots. \tag{113}$$

Comparison with a numerical evaluation for $k = 0, \ldots, 5$ shows that the error of the approximation is about 10% for $a = 1$, 1% for $a = 5$ and 0.1% for $a = 10$. Hence, for large a (which we have) the formula (112) should work very well.

Having gained sufficient confidence in our saddle point approximation we rewrite the imaginary part of (40) using (91),

$$\operatorname{Im} P_\pm \simeq \frac{\alpha}{6\pi^{1/2}}\kappa^{-3/2}\sum_{k\geqslant 0}(-1)^k A_k\{2I(a, k-1/2) + (1\pm 3)I(a, k+1/2)\}, \tag{114}$$

with A_k as defined in (94). Employing our integration formula (112) we find

$$\operatorname{Im} P_\pm \simeq \frac{\alpha}{24}\sqrt{\frac{3}{2}}\frac{1}{\kappa}\,\mathrm{e}^{-8/3\kappa}\sum_{k\geqslant 0} B_{k\pm}\left(-\frac{3\kappa}{8}\right)^k, \tag{115}$$

where the new expansion coefficients are given by the somewhat lengthy expression

$$B_{k\pm} \equiv A_k \left\{ \frac{9 \pm 3}{4} + \frac{72k}{(6k-7)(6k+1)} \left[\frac{9 \pm 3}{4}(k-1) + \frac{-7 \pm 3}{8} \right] \right\}. \tag{116}$$

Admittedly, this is not too illuminating so we evaluate the series (115) to order κ^2 or $(\epsilon\nu)^2$ and use (89) to determine

$$\operatorname{Im} \Delta_\pm \simeq N_{\pm,\mathrm{sp}} \frac{\alpha\epsilon^2}{90} \frac{4}{3\epsilon\nu} \mathrm{e}^{-4/3\epsilon\nu} \left\{ 1 + \frac{25 \mp 12}{72} \frac{3\epsilon\nu}{4} + \frac{265 \mp 168}{2 \times 72^2} \left(\frac{3\epsilon\nu}{4} \right)^2 \ldots \right\}. \tag{117}$$

In the above we have introduced the saddle point normalization factor[9]

$$N_{\pm,\mathrm{sp}} \equiv (3 \pm 1) \tfrac{45}{32} \sqrt{\tfrac{3}{2}}. \tag{118}$$

We refrain from identifying this with the analogous factor in (110) as the approximation schemes involved do not allow for a direct comparison of the normalization. The latter will be fixed in a moment by means of the dispersion relation (83).

Putting these niceties aside we stress that we find perfect agreement between (110) and (117) concerning the LO dependence on powers of $\epsilon\nu$ and the nonperturbative exponential. The only discrepancy resides in the τ-coefficients multiplying the sub-leading terms of order $\epsilon\nu$. In view of the fairly different approximations employed this is probably not too surprising.

6. Discussion and conclusion

With the consequences of our large-order analysis confirmed analytically we can go even one step further. We can use the Kramers–Kronig relation (83) to actually *define* the real part of the indices of refraction nonperturbatively, i.e. without relying on the derivative expansion. To this end we take the leading order of the imaginary part (110) or (117) as a *model* by writing

$$\operatorname{Im} \Delta_\pm(\epsilon, \nu) = N_\pm \frac{\alpha\epsilon^2}{90} \frac{4}{3\epsilon\nu} \mathrm{e}^{-4/3\epsilon\nu}. \tag{119}$$

Plugging this into the dispersion relation (83) we can actually perform the principal value integral analytically with the result

$$\operatorname{Re} \Delta_\pm = N_\pm \frac{\alpha\epsilon^2}{90\pi} \frac{4}{3\epsilon\nu} \{ \mathrm{Ei}(4/3\epsilon\nu)\, \mathrm{e}^{-4/3\epsilon\nu} - \mathrm{Ei}(-4/3\epsilon\nu)\, \mathrm{e}^{4/3\epsilon\nu} \}. \tag{120}$$

Matching the perturbative small-$\epsilon\nu$ behaviour fixes the normalization to be

$$N_\pm = 11 \pm 3. \tag{121}$$

Interestingly, in (120) exponential integrals Ei appear multiplied by exponentials, constituting a paradigm example of functions displaying factorial growth expansion coefficients. With the real part thus determined we summarize our findings in figure 7 which shows both real and imaginary parts of Δ_+ as a function of frequency ν for fixed $\epsilon^2 = 0.1$. We have added the series expansion to second order (the full line of figure 1) which coincides well with the exact real part for small ν where the factorial growth is not visible yet.

The graph for Δ_- looks almost identical with a slight shift in the vertical scale due to the difference in normalization. Hence, we refrain from producing an extra plot.

By construction, the real and imaginary parts of Δ (thus also of $n = 1 + \Delta$) are related by the Kramers–Kronig relation (83) with $\operatorname{Im} n \neq 0$ signalling absorption, i.e. pair production.

[9] The leading term in (117) has already been determined by Ritus [11]. His normalization differs from ours by a factor of 2, a discrepancy we have not been able to trace. The most plausible explanation seem to be the ambiguities in determining the prefactor in the saddle point approximation.

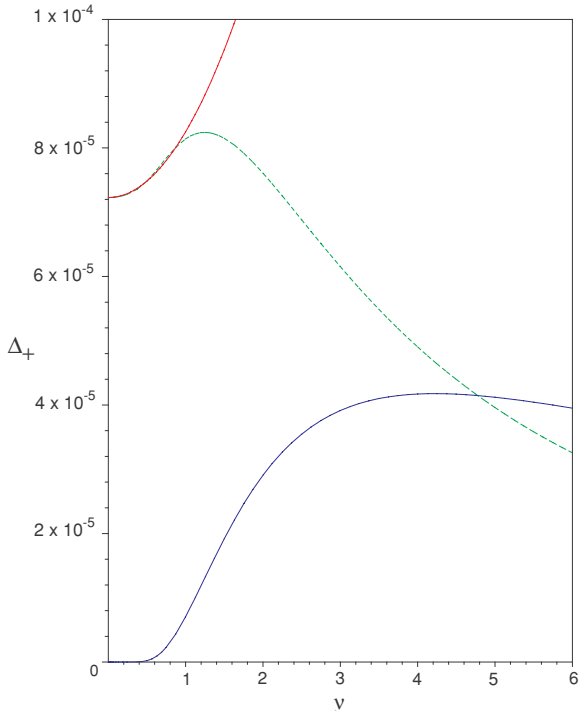

Figure 7. Real and imaginary parts of the deviation Δ_+ of the index n_+ from unity (dashed and lower full curve, respectively). The upper full curve bending upwards is the series expansion of Δ_+ to second order (same curve as in figure 1).

By looking at figure 7 we see that the latter sets in roughly at the critical value of $\nu = 1$. Here, $\mathrm{Re}\, n$ attains its maximum and decreases for $\nu \gtrsim 1$ while $\mathrm{Im}\, n$ increases. Mathematically, we may state

$$\begin{aligned} \frac{\partial\, \mathrm{Re}\, n_\pm}{\partial \omega} &> 0 \qquad \text{for} \quad \omega \ll m_e, \quad \text{(normal dispersion)} \\ \frac{\partial\, \mathrm{Re}\, n_\pm}{\partial \omega} &< 0 \qquad \text{for} \quad \omega \gtrsim m_e, \quad \text{(anomalous dispersion)} \end{aligned} \tag{122}$$

where we have reinstated physical units (recall that ω is the probe frequency). We conclude that it is a consequence of the Kramers–Kronig relations based on the fundamental principle of causality that absorption is intimately connected to anomalous dispersion.

The physics involved can be wrapped up as follows. We have analysed the influence of crossed background fields on the propagation of light (e.g. laser beams). Using exact integral representations for the eigenvalues of the polarization tensor we found that to all orders in probe frequency and background intensity there is birefringence of the vacuum induced by the crossed background fields. The effect can be described in terms of background-dependent effective metrics $h_\pm^{\mu\nu}$ implying dispersion relations $h_\pm^{\mu\nu} k_\mu k_\nu = 0$ which describe distorted light cones. Solving for the indices of refraction $n_\pm$ one finds that they are frequency dependent, starting out with normal dispersion. At critical energy and intensity anomalous dispersion sets in together with absorption due to pair production.

At present an experiment is being designed that plans to measure vacuum birefringence using a high-power laser background probed by x-ray beams [6]. The experiment is quite demanding as one has to measure ellipticity signals with a sensitivity at the order of 10^{-11} for presently available probes and lasers. As the signal is proportional to $\nu^2\epsilon^4$ it may be readily enhanced by increasing probe frequency and background intensity. Within the next few years one expects a reduction of the required sensitivity down to 10^{-4}. Normal dispersion is an NLO effect; hence implies a signal of order $\nu^4\epsilon^4$ requiring a sensitivity of 10^{-8} within the envisaged scenario. This is still within the theoretical limits of measurability [39]. Pair production shows up in terms of a nonvanishing imaginary part or as anomalous dispersion of the real part. To become observable both effects require parameters ν and ϵ close to their critical values. For instance, if $\epsilon \simeq 10^{-2}$ then $\mathrm{Im}\,\Delta \simeq 10^{-11}$ for $\nu \simeq 0.8$. Even these moderate values cannot be attained at present so that it is presumably more reasonable to look for positrons rather than optical signals to detect pair production.

From a theorist's point of view one should also consider two-loop corrections and the influence of nonconstant backgrounds. The two-loop corrections to the Heisenberg–Euler Lagrangian (cf appendix) have been calculated by Ritus [40]. They amount to a replacement of the LO coefficients of (71) according to

$$\begin{Bmatrix} 14 \\ 8 \end{Bmatrix} \to \begin{Bmatrix} 14(1+1315\alpha/252\pi) \\ 8(1+40\alpha/9\pi) \end{Bmatrix}. \tag{123}$$

These are both one-percent corrections to the LO $= O(\nu^0)$ behaviour in (71).

Regarding nonconstant backgrounds it is possible to slightly relax the crossed-field assumption in a perfectly controlled manner. Laser beams may be more realistically described as *Gaussian beams* rather than plane waves. The former have a Gaussian profile in transverse direction of 'waist size' w_0 and a Lorentz profile in the longitudinal direction characterized by the 'Rayleigh length' z_0. One can form the small dimensionless parameter $\triangle \equiv w_0/2z_0 \ll 1$ [41] which describes the deviation from the crossed-field limit corresponding to $\triangle = 0$. Naturally, one expects that there will be $O(\triangle)$-corrections to the results presented here.

It is this context of nonconstant backgrounds where the intuition gained in this paper is expected to pay off. In this more realistic case, we cannot hope to have any exact analytical results available. Thus it is important to know both the region of validity and the limitations of derivative and weak-field expansions. From our results they are both expected to break down if the product of frequency squared and intensity becomes $\omega^2 I = O\left(m_e^6/e^2\right)$, or, in dimensionless units, $\epsilon^2\nu^2 = O(1)$ (see figure 7). With the present values of $\epsilon^2\nu^2 \simeq 10^{-13}$ and those expected in the near future ($\epsilon^2\nu^2 \simeq 10^{-10}$), however, one is definitely on the safe side where (asymptotic) expansion methods make perfect sense.

Acknowledgments

It is a pleasure to thank Arsen Khvedelidze, Martin Lavelle, David McMullan, Paul Rakow, Roland Sauerbrey, Igor Shovkovy and Andreas Wipf for very useful discussions. This research was carried out while OS was a PPARC postdoctoral research fellow at the University of Plymouth.

Appendix. Heisenberg-Euler analysis

In this appendix we will check our LO results (59) and (60) in an independent manner by using the Heisenberg–Euler (HE) effective Lagrangian [42, 43]. This is the LO in the derivative

expansion of the effective action (5) but contains all orders in the intensity. It has the well-known proper-time representation [4] (we follow the nice review [9])

$$\delta\mathscr{L} = -\frac{1}{8\pi^2}\int_0^\infty \frac{\mathrm{d}s}{s}\,\mathrm{e}^{-seE_c}\left\{\frac{e^2\mathfrak{a}\mathfrak{b}s^2}{\tanh(e\mathfrak{b}s)\tan(e\mathfrak{a}s)} - 1 - \frac{e^2s^2}{3}(\mathfrak{a}^2-\mathfrak{b}^2)\right\}, \tag{A.1}$$

and is exact for constant fields but remains approximately valid for photon frequencies small compared to the electron mass as in (12). The quantities $\pm\mathrm{i}\mathfrak{a}$ and $\pm\mathfrak{b}$ are the eigenvalues of the constant matrix

$$G_{\mu\nu} \equiv F_{\mu\nu} + f_{\mu\nu}, \tag{A.2}$$

consisting of both background and probe field. They are related to the standard scalar and pseudoscalar invariants defined in (22) and (23) via

$$\mathfrak{a}^2 - \mathfrak{b}^2 = -\tfrac{1}{2}G_{\mu\nu}G^{\mu\nu} \equiv 2\mathscr{S}, \tag{A.3}$$

$$\mathfrak{a}\mathfrak{b} = -\tfrac{1}{4}G_{\mu\nu}\tilde{G}^{\mu\nu} \equiv \mathscr{P}. \tag{A.4}$$

Note that in this appendix the invariants $\mathscr{S}$ and $\mathscr{P}$ denote the contribution of *both* background and fluctuation, cf (A.2), and thus are nonvanishing. The representation (A.1) contains all orders in the field $G_{\mu\nu}$. Low intensities allow for a weak-field expansion the first two orders of which are

$$\delta\mathscr{L} = \frac{\alpha^2}{m_e^4}\left(\frac{8}{45}\mathscr{S}^2 + \frac{14}{45}\mathscr{P}^2\right) + \frac{\alpha^3}{m_e^8}\left(\frac{256\pi}{315}\mathscr{S}^3 + \frac{416\pi}{315}\mathscr{S}\mathscr{P}^2\right). \tag{A.5}$$

It is worth pointing out that exactly the same numerical coefficients appear as in (71).

For what follows it is useful to write the LO of (A.5) as

$$\delta\mathscr{L} = \tfrac{1}{2}\gamma_-\mathscr{S}^2 + \tfrac{1}{2}\gamma_+\mathscr{P}^2 + O(\alpha^3), \tag{A.6}$$

with the couplings $\gamma_\pm$ given by

$$\gamma_+ \equiv 7\xi, \qquad \gamma_- \equiv 4\xi, \qquad \xi \equiv \frac{\alpha}{45\pi}\frac{1}{E_c^2}. \tag{A.7}$$

To approximate the polarization tensor $\Pi^{\mu\nu}$ we start from (A.5), decompose into background F and probe f according to (A.2) and expand the HE action, $\delta S = \int \mathrm{d}^4x\,\delta\mathscr{L}$, to second order in the probe field f,

$$\delta S[F, f] = \tfrac{1}{8}(f_{\alpha\beta}, \Omega^{\alpha\beta\mu\nu}f_{\mu\nu}). \tag{A.8}$$

The tensor $\Omega^{\alpha\beta\mu\nu}$ is proportional to the second derivative of $\delta\mathscr{L}$,

$$\Omega^{\alpha\beta\mu\nu} \equiv 4\,\frac{\partial^2(\delta\mathscr{L})}{\partial f_{\alpha\beta}\partial f_{\mu\nu}}\bigg|_{f=0}. \tag{A.9}$$

So far we have not exploited the fact that our background consists of crossed fields. Note that the derivative in (A.9) is evaluated right at the background. It is easy to see that enormous simplifications arise in the crossed-field case due to the vanishing of the background invariants. The generic term in the HE Lagrangian is of the form $\mathscr{S}^n\mathscr{P}^{2m}$ (as odd powers of $\mathscr{P}$ are forbidden by CP invariance) with n and m integers. Taking the two derivatives in (A.9) at $f = 0$ one will always end up with (vanishing) powers of $\mathscr{S}$ and $\mathscr{P}$ unless n and m are sufficiently small. The only surviving cases turn out to be the Maxwell term, $(n = 1, m = 0)$, and the LO (A.6) with $n = 2$, $m = 0$ and $n = 0$, $m = 1$. Thus, for crossed fields, the effective Lagrangian (A.1) gets truncated after the LO α^2/m_e^4. In other words, the LO describes the

exact dependence on intensity for crossed-field background[10]! In view of these considerations the tensor $\Omega^{\mu\nu\alpha\beta}$ simplifies to

$$\Omega^{\mu\nu\alpha\beta} = \gamma_- F^{\alpha\beta} F^{\mu\nu} + \gamma_+ \tilde{F}^{\alpha\beta} \tilde{F}^{\mu\nu}. \tag{A.10}$$

Note that it is symmetric upon exchanging $(\mu\nu) \leftrightarrow (\alpha\beta)$ and antisymmetric both in μ and ν as well as α and β.

In momentum space the polarization tensor $\Pi^{\mu\nu}$ is then given by contracting (A.10) twice with the wave vector k associated with the probe field $f_{\mu\nu}$,

$$\Pi^{\mu\nu}(k) \equiv \Omega^{\mu\alpha\nu\beta} k_\alpha k_\beta = \gamma_- b^\mu b^\nu + \gamma_+ \tilde{b}^\mu \tilde{b}^\nu. \tag{A.11}$$

To LO in k^2 this coincides with (21) as it should, the nonvanishing eigenvalues being given by $\Pi_\pm = \gamma_\pm b^2(k)$. They imply the dispersion relations,

$$k^2 - \gamma_\pm b^2(k) = 0 \tag{A.12}$$

and effective metrics

$$h_\pm^{\mu\nu} = g^{\mu\nu} + \gamma_\pm T^{\mu\nu}. \tag{A.13}$$

Introducing the index n of refraction according to (4) the dispersion relations (A.12) and (A.13) become four quadratic equations for n. Demanding $n = 1$ for $\gamma_\pm = 0$ singles out two of them. These are conveniently written in terms of the abbreviations (29)–(31),

$$n_\pm = \frac{1}{1 - \gamma_\pm(\mathcal{H} - \mathcal{H}_k)} \left\{ \sqrt{1 + \gamma_\pm \mathcal{H}_k - \gamma_\pm^2 [\mathcal{H}^2 - (\mathbf{k}\cdot\boldsymbol{S})^2 - \mathcal{H}\mathcal{H}_k]} - \gamma_\pm \mathbf{k}\cdot\boldsymbol{S} \right\} \tag{A.14}$$

and have the small-$\gamma_\pm$ expansion,

$$n_\pm = 1 + \gamma_\pm(\mathcal{H} - \mathbf{k}\cdot\boldsymbol{S} - \mathcal{H}_k/2) + \tfrac{1}{2}\gamma_\pm^2 [(\mathcal{H} - \mathbf{k}\cdot\boldsymbol{S} - \mathcal{H}_k)^2 - \mathcal{H}_k/2] + \cdots. \tag{A.15}$$

For a head-on collision of probe and background (A.14) yields the simple expression

$$n_\pm = \frac{1 + \gamma_\pm I}{1 - \gamma_\pm I} = 1 + \frac{2\gamma_\pm I}{1 - \gamma_\pm I} \equiv 1 + \Delta_\pm, \tag{A.16}$$

which is exact to all orders in the intensity I. Noting that

$$\gamma_\pm I = \frac{11 \pm 3}{2} \frac{\alpha\epsilon^2}{45\pi}, \tag{A.17}$$

the result (A.16) coincides with (59) and (60).

References

[1] Tajima T and Mourou G 2002 Zettawatt-exawatt lasers and their applications in ultrastrong-field physics *Phys. Rev. Spec. Top. Accel. Beams* **5** 031301

[2] Hein J, Podleska S, Siebold M, Hellwing M, Bödefeld R, Sauerbrey R, Ehrt D and Winzer W 2004 Diode-pumped chirped pulse amplification to the joule level *Appl. Phys.* B **79** 419

[3] see e.g. the XFEL-STI interim report at http://xfel.desy.de/

[4] Schwinger J 1951 On gauge invariance and vacuum polarization *Phys. Rev.* **82** 664

[5] Sauter F 1931 Über das Verhalten eines Elektrons im homogenen elektrischen Feld nach der relativistischen Theorie Diracs *Z. Phys.* **69** 742

[6] Heinzl T, Liesfeld B, Amthor K U, Schwoerer H, Sauerbrey R and Wipf A 2006 On the observation of vacuum birefringence *Opt. Commun.* (at press) (*Preprint* hep-ph/0601076)

[7] Brezin E and Itzykson C 1970 Polarization phenomena in vacuum nonlinear electrodynamics *Phys. Rev.* D **3** 618

[8] Dittrich W and Gies H 2000 *Probing the Quantum Vacuum (Springer Tracts Mod. Phys.* vol 166*)* (Berlin: Springer)

[9] Dunne G V 2004 Heisenberg–Euler effective Lagrangians: basics and extensions *Preprint* hep-th/0406216

[10] An analogous observation has been made for photon splitting in a plane-wave field [15].

[10] Narozhnyi N B 1968 Propagation of plane electromagnetic waves in a constant field *Zh. Eksp. Teor. Fiz.* **55** 714–21
Narozhnyi N B 1969 *Sov. Phys.—JETP* **28** 371
[11] Ritus V I 1972 Radiative corrections in quantum electrodynamics with intense field and their analytical properties *Ann. Phys.* **69** 555
[12] Becker W and Mitter H 1975 Vacuum polarization in laser fields *J. Phys. A: Math. Gen.* **8** 1638
[13] Schwoerer H, Liesfeld B, Schlenvoigt H-P, Amthor K-U and Sauerbrey R 2006 Thomson-backscattered x-rays from laser-accelerated electrons *Phys. Rev. Lett.* **96** 014802
[14] Ringwald A 2003 Boiling the vacuum with an x-ray free electron laser *Preprint* hep-ph/0304139
[15] Affleck I and Kruglyak L 1987 Photon splitting in a plane wave field *Phys. Rev. Lett.* **59** 1065
[16] Białynicka-Birula Z and Białynicki-Birula I 1970 Nonlinear effects in quantum electrodynamics. Photon propagation and photon splitting in an external field *Phys. Rev.* D **2** 2341
[17] Abramowitz M and Stegun I A (ed) 1970 *Handbook of Mathematical Functions (With Formulas, Graphs, and Mathematical Tables)* 9th edn (New York: Dover)
[18] http://dlmf.nist.gov/
[19] Peskin M E and Schroeder D V 1995 *An Introduction to Quantum Field Theory* (Reading, MA: Addison-Wesley)
[20] Novello M, De Lorenci V A, Salim J M and Klippert R 2000 Geometrical aspects of light propagation in nonlinear electrodynamics *Phys. Rev.* D **61** 045001
[21] Liberati S, Sonego S and Visser M 2001 Scharnhorst effect at oblique incidence *Phys. Rev.* D **63** 085003
[22] Zavattini E *et al* 2006 Experimental observation of optical rotation generated in vacuum by a magnetic field *Phys. Rev. Lett.* **96** 110406
[23] Toll J 1952 The dispersion relation for light and its application to problems involving electron pairs *PhD Thesis* Princeton
[24] McDonald K T 1986 Proposal for experimental studies of nonlinear quantum electrodynamics *Preprint* DOE/ER/3072-38. Available at http://www.hep.princeton.edu/mcdonald/e144/prop.pdf
[25] Baier R and Breitenlohner P 1967 *Acta Phys. Austriaca* **25** 212
[26] Baier R and Breitenlohner P 1967 *Nuovo Cimento* B **47** 117
[27] Adler S L 1971 Photon splitting and photon dispersion in a strong magnetic field *Ann. Phys.* **67** 599–647
[28] Dunne G V and Hall T M 1999 Borel summation of the derivative expansion and effective actions *Phys. Rev.* D **60** 065002
[29] Rakow P E L 2005 Stochastic perturbation theory and the gluon condensate *PoS* **LAT2005** 284
[30] Gies H and Langfeld K 2002 Loops and loop clouds: a numerical approach to the worldline formalism in QED *Int. J. Mod. Phys.* A **17** 966
[31] Gies H and Langfeld K 2001 Quantum diffusion of magnetic fields in a numerical worldline approach *Nucl. Phys.* B **613** 353
[32] Gies H, Sanchez-Guillen J and Vazquez R A 2005 Quantum effective actions from nonperturbative worldline dynamics *J. High Energy Phys.* JHEP08(2005)067
[33] Gies H and Klingmüller K 2005 Pair production in inhomogeneous fields *Phys. Rev.* D **72** 065001
[34] Dunne G V 2002 Perturbative-nonperturbative connection in quantum mechanics and field theory *Preprint* hep-th/0207046
[35] Bjorken J D and Drell S D 1965 *Relativistic Quantum Field Theory* (New York: McGraw-Hill)
[36] Lobanov A E, Rodionov V N, Ternov I M and Khalilov V R 1980 Amplitudes of elastic scattering of electrons and photons in a constant electromagnetic field *Teor. Mat. Fiz.* **45** 377
Lobanov A E, Rodionov V N, Ternov I M and Khalilov V R 1981 *Theor. Math. Phys.* **45** 1089 (Engl. Transl.)
[37] Di Piazza A, Hatsagortsyan K Z and Keitel C H 2006 Light diffraction by a strong standing electromagnetic wave *Preprint* hep-ph/0602039
[38] Gil A, Segura J and Temme N N 2002 GIZ, HIZ: two Fortran 77 routines for the computation of complex Scorer functions *ACM Trans. Math. Soft.* **28** 436
[39] Alp E E, Sturhahn W and Toellner T S 2000 Polarizer-analyzer optics *Hyperfine Interact.* **125** 45
[40] Ritus V I 1976 *Sov. Phys.—JETP* **42** 774
[41] Bulanov S S, Narozhny N B, Mur V D and Popov V S 2004 On e^+e^--pair production by a focused laser pulse in vacuum *Phys. Lett.* A **330** 1
[42] Heisenberg W and Euler H 1936 Folgerungen aus der Diracschen Theorie des Positrons *Z. Phys.* **98** 714–32
[43] Weisskopf V 1936 Über die Elektrodynamik des Vakuums auf Grund der Quantentheorie des Elektrons *K. Dan. Vidensk. Selsk. Mat. Fys. Medd.* **14** 6 (reprinted in *Quantum Electrodynamics* 1958 ed J Schwinger (New York: Dover))